Korean J. Chem. Eng., **26**(3), 856-861 (2009)

Thermogravimetric analysis and pyrolysis of waste mixtures of paint and tar slag

Ling Tao†, Guang-Bo Zhao, Juan Qian, and Yu-Kun Qin

School of Energy Science and Engineering, Harbin Institute of Technology, 92, West Dazhi Street, Harbin 150001, P. R. China
(*Received 19 July 2008 • accepted 18 November 2008*)

Abstract–We describe thermogravimetric analyses and pyrolysis kinetic studies carried out on hazardous waste mixtures of tar slag, paint slag, paper, sodium sulfate and calcium oxide. Both thermogravimetric (TG) and differential thermogravimetric (DTG) profiles were measured by a thermogravimetric analyzer at different final temperatures, particle sizes and heating rates. Pyrolysis kinetic parameters were calculated by the Coats-Redfern method. Influences of particle size, heating rate and final temperature on pyrolysis yields and kinetic parameters are also discussed. The results show that final temperature and particle size have a great effect on pyrolysis yields. We find that with increasing temperature the activation energy initially increases to a maximum value and then decreases.

Key words: Thermogravimetric Analysis, Hazardous Waste, Pyrolysis Kinetics, Paint Slag, Tar Slag

INTRODUCTION

Hazardous waste from industrial production has become an ever increasing concern accompanying economic development. It has been estimated that about 10 million tons of hazardous wastes are produced annually in China [1-5]. There is a wide variety of hazardous industrial waste, most of which is harmful and very slow to decompose naturally. The various wastes cause great damage to biological life and environment, and it is a matter of urgency to develop treatments to process wastes in a proper way.

In much of the world, resource utilization, minimization and harmless treatment are prominent methods used in disposing of hazardous waste. In China, for the present, the harmless treatment is the most suitable method, and one such method, incineration, is widely used because of its decrement, disinfection and low levels of secondary pollution [6,7]. Pyrolysis is the leading process of incineration and for this reason this process should be studied more deeply to gain a better understanding of incineration kinetics. Pyrolysis of solid wastes is a thermo-chemical process, which can decompose wastes into solid residues of smaller molecules and combustible gases into inert gases, all as a consequence of the poor thermo-stability of organic components of wastes. Thermogravimetry is widely used in studying coal and biomass pyrolysis characteristics and its reaction mechanism, but is seldom used in pyrolysis of hazardous wastes. In this paper, we describe experiments carried out by non-isothermal thermogravimetry of the pyrolysis characteristics of hazardous wastes derived from paint and tar. Effects of particle size, heating rate, and finish temperature on pyrolysis kinetics are discussed.

EXPERIMENTAL DESCRIPTION

1. Specimen and Instrumentation

Specimens of hazardous wastes were provided by the Shanghai LüZou Environmental Protection Engineering Company. The composition of these specimens were paint slag (40%), tar slag (35%), $NaSO_4$ (10%), CaO (5%) and paper (10%). Mixtures of wastes were ground into powder within four ranges of particle sizes, <0.1 mm, 0.1-.25 mm, 0.25-0.6 mm, and 0.6-1 mm, and identified simply as 0001, 0125, 2560 and 0610, respectively. Table 1 provides the elemental composition and heat value of each specimen.

Table 1. Elemental composition and heat value of the specimen

C_{ar} (%)	H_{ar} (%)	O_{ar} (%)	N_{ar} (%)	S_{ar} (%)	M_{ar} (%)	A_{ar} (%)	$Q_{net,ar}$ (kJ/kg)
47.87	3.55	6.66	0.81	0.28	19.88	20.95	18874.22

We used a METTLER-TOLEDO thermogravimetric analyzer TGA/SDTA851^e for which the maximum operating temperature is 1,600 °C, the maximum heating rate is 100 °C/min, and the maximum temperature fluctuation is 0.25 °C. The full-scale mass range is 2 g with a mass resolution of 0.1 μg. The specimen temperature sensor is positioned under the crucible holder and was calibrated with a pure metal standard sample throughout the whole measurement procedure. The Al_2O_3 crucible is 12 mm in diameter with a volume of 150 μL. A thermostat controls the temperature of balance housing and cooling of the hot furnace. The temperature setting of the thermostat was maintained at 22 °C with a coolant flow rate of 200 mL/min.

2. Experimental Method

Nitrogen with purity of 99.999% and flow rate of 30 mL/min was used as a protective gas, and as a reactive gas when delivered at the flow rate of 130 mL/min. The mass of the samples was prescribed at about 120 mg. Before the experiment was started, the furnace was purged for about 30 minutes at 40 °C. The furnace was then heated from 40 °C to 105 °C at a heating rate of 20 °C/min and held at 105 °C for 10 minutes to evaporate external moisture. The furnace was subsequently heated from 105°C to its final temperature at a 50 °C/min rate and held at this final temperature for 20 minutes. Final temperatures chosen were 800 °C, 900 °C, 1,000 °C, 1,100 °C and 1,200 °C. Experiments on specimen 2560 were performed at

†To whom correspondence should be addressed.
E-mail: taolingsd@yahoo.com.cn
‡This work was presented at the 7th China-Korea Workshop on Clean Energy Technology held at Taiyuan, Shanxi, China, June 26-28, 2008.

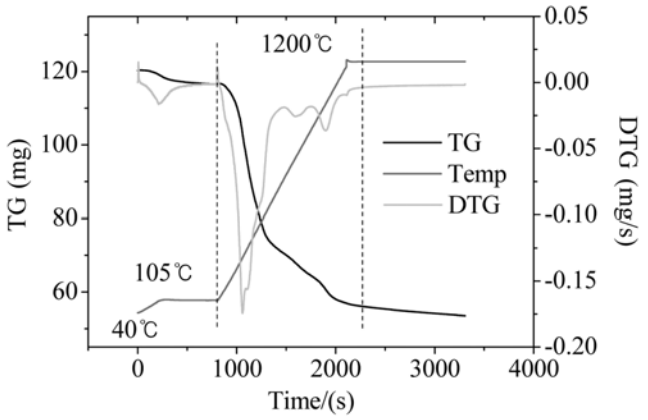

Fig. 1. TG/DTG profiles for test condition 2560-50-1200.

heating rates of 20 ℃/min, 50 ℃/min and 80 ℃/min. Below, run conditions for each experimental run of a specimen are referred to in the format "particle size-heating rate-final temperature."

RESULTS AND DISCUSSION

1. Weight Loss Characteristics

The TG/DTG profiles of test condition 2560-50-1200 are presented in Fig. 1. The pyrolysis of wastes can be divided into three stages. The first stage corresponds to a heating period from 40 ℃ to 105 ℃ and constant temperature regime of 105 ℃ during which the specimen loses its external moisture. A second heating period from 105 ℃ to 1,200 ℃ with the heating rate of 50 ℃/min is the main pyrolysis stage with a large gas release. The constant temperature stage at 1,200 ℃ is the residual pyrolysis stage and is accompanied by a small amount of weight loss. From the DTG profile, we find that there are three obvious peaks in the main pyrolysis stage corresponding to temperatures of 302.3 ℃, 752.2 ℃ and 1079.4 ℃.

2. Characteristic Temperature

The various temperatures associated with i) the initial weight loss (T_{il}), ii) the initial pyrolysis (T_{ip}), iii) the maximum weight loss rate (T_{max}), and iv) the final temperature (T_f), can be obtained from the TG and DTG profiles. The initial weight loss temperature and final temperature are separately defined as the temperature for which the weight loss rate reaches 0.025 mg/s for the first and last times, respectively. The initial pyrolysis temperature is defined as the temperature corresponding to the point of intersection of the tangent associated with the largest weight loss rate on the TG profile and the extended line of the plateau. These four temperatures are collectively called the characteristic temperatures.

It is obvious in Figs. 2-5 that particle size has a significant effect on characteristic temperatures of pyrolysis. Characteristic temperatures rise with increasing particle size because the specific surface area decreases and conduction weakens with increasing particle size, especially at low temperatures when the crucible absorbs weak radiation from the furnace. However, with increasing particle size, the specific surface area decreases, and therefore the convection energy from reactive and protective gases is lessened. Conduction would remain as the main means the internal temperature is raised; weak conduction makes the temperature difference between inside and outside of the crucible even larger, which creates a lag in weight loss in the middle of the crucible.

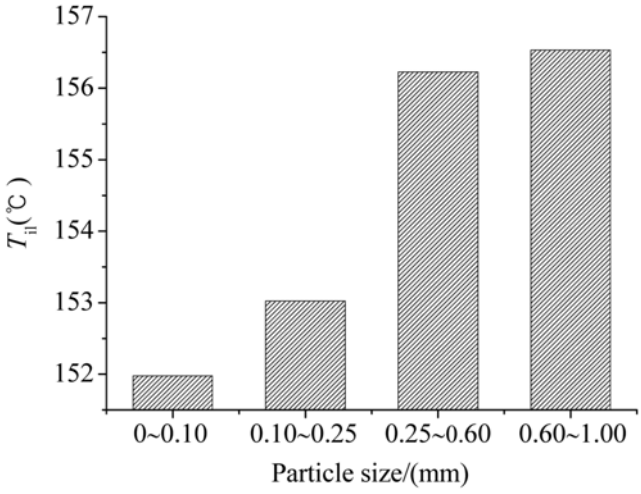

Fig. 2. Initial weight loss temperatures for various particle sizes.

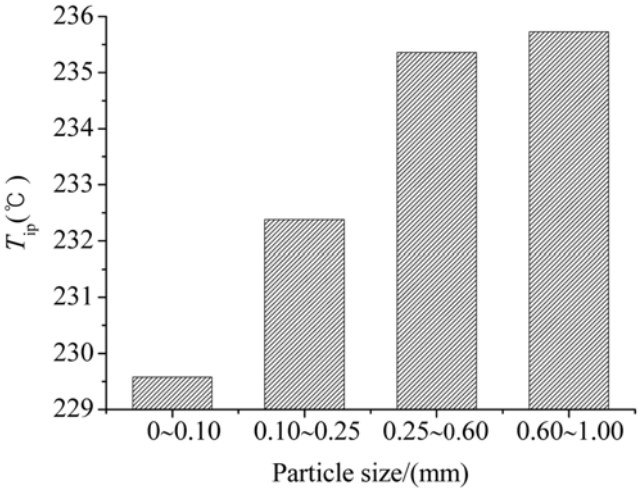

Fig. 3. Initial pyrolysis temperatures for various particle sizes.

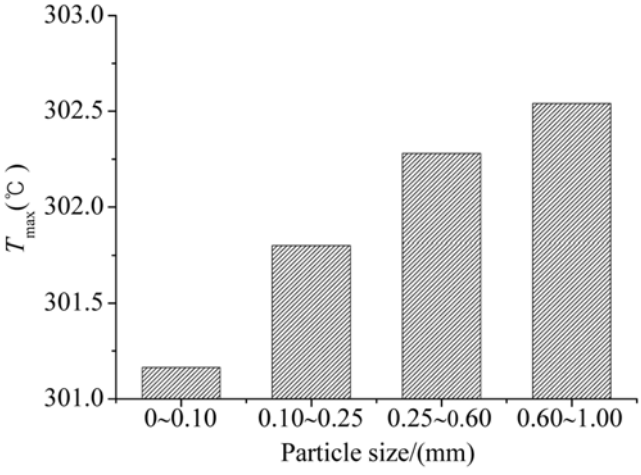

Fig. 4. Maximum weight loss rate temperatures for various particle sizes.

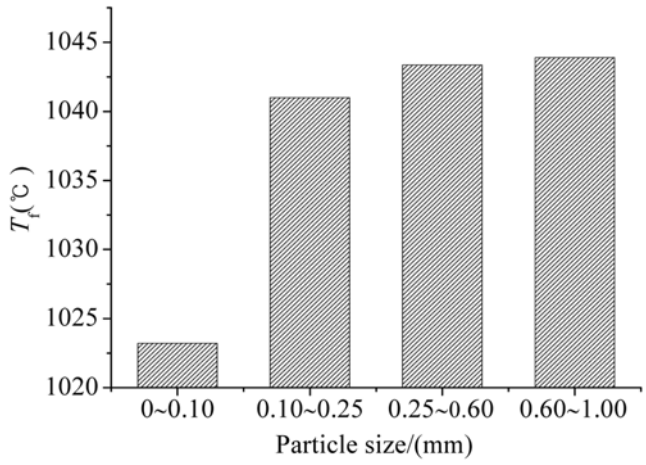

Fig. 5. Final temperatures for various particle sizes.

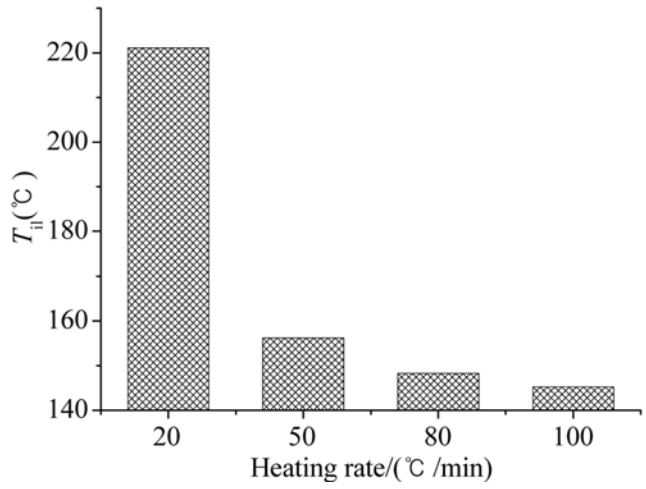

Fig. 6. Initial weight loss temperatures for various heating rates.

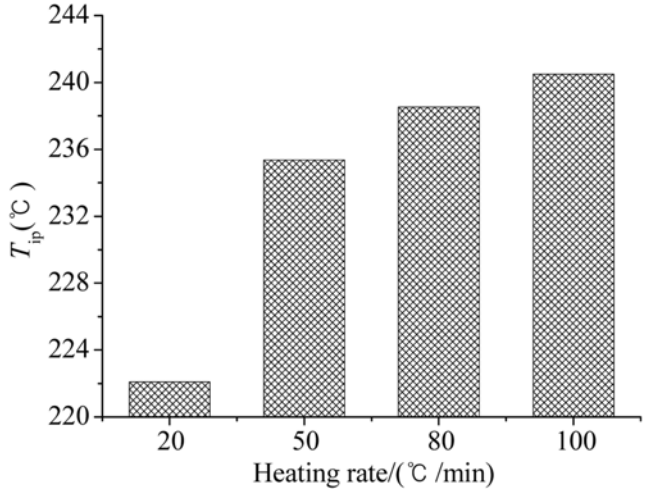

Fig. 7. Initial pyrolysis temperatures for various heating rates.

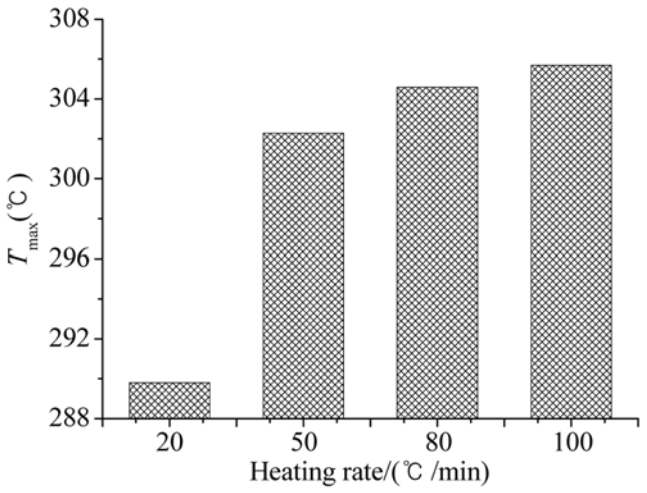

Fig. 8. Maximum weight loss rate temperatures for various heating rates.

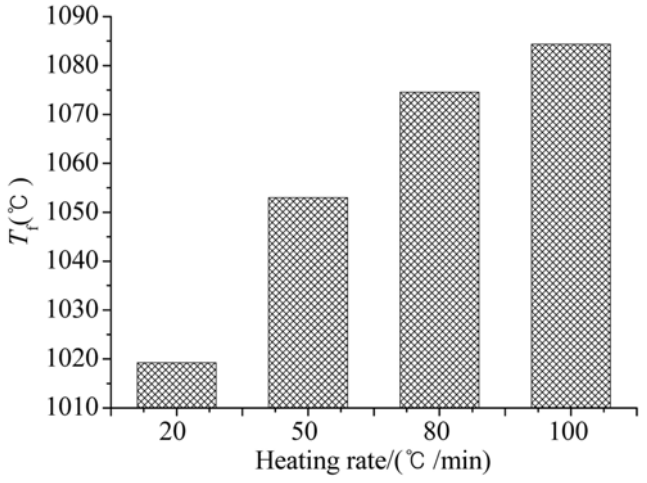

Fig. 9. Final temperatures for various heating rates.

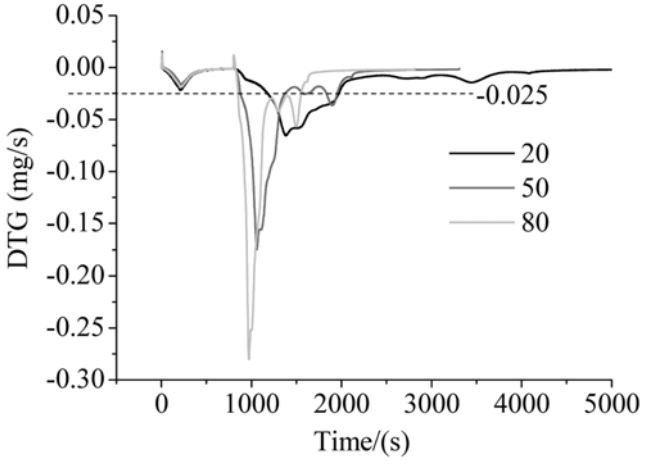

Fig. 10. DTG profiles for various heating rates.

Figs. 3-9 show the characteristic temperatures of specimen 2560 from which it is evident that these temperatures clearly change with heating rate. The pyrolysis time shortens with increasing heating rate, which promotes more weight loss in unit time. Therefore higher heating rate conditions reach the initial weight loss temperature much

earlier than lower heating rate conditions do, as shown in Fig. 6. The temperature increase of the crucible and specimen surface rises rapidly with increasing heating rate as in Fig. 10 [8]. However, due to the limitation of thermo conductivity, a thermal gradient is formed between the surface and the middle. The higher the heating rate, the lower the temperature becomes. Temperature hysteresis produces pyrolysis hysteresis, thereby raising the characteristic temperature.

3. Pyrolysis Yield

Fig. 11 presents the pyrolysis yields of different final temperatures and shows that these temperatures have a great influence on pyrolysis yields. It can be seen in Fig. 12 that polycondensation cannot react completely due to the low final temperature of 800 ℃, while it can basically come to completion at 900 ℃. A secondary reaction occurs at 1,000 ℃, producing partial yields while at 1,100 ℃ yields are complete [9]. Therefore, changes between 1,100 and 1,200 ℃ are smaller than those between 800 ℃, 900 ℃ and 1,000 ℃.

Fig. 13 presents the pyrolysis yield profiles for various particle sizes, and establishes the fact that yields increase with increasing particle size. Smaller particle size corresponds to larger bulk density and smaller clearance [10], and hence the volatile component cannot separate out in time, creating a local volatile atmosphere hindering the reaction. The larger the particle size, the larger the clearance is, and therefore the volatile component separates out in time and the pyrolysis yield rises.

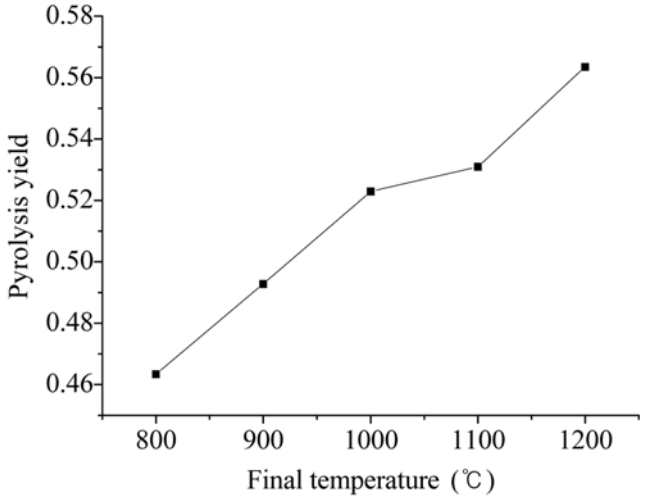

Fig. 11. Pyrolysis yields for various final temperatures.

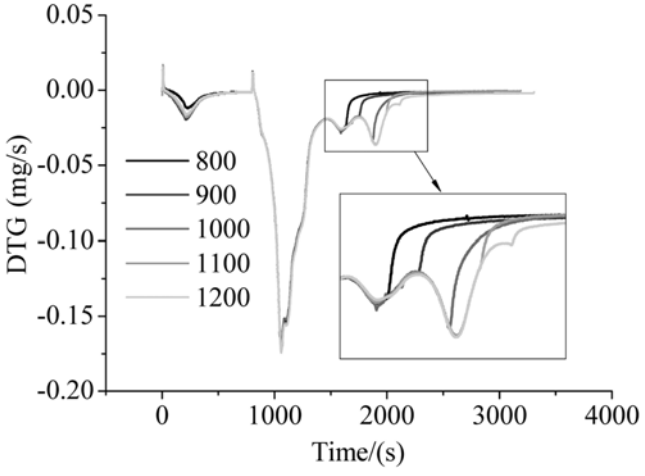

Fig. 12. DTG profiles for various heating rates.

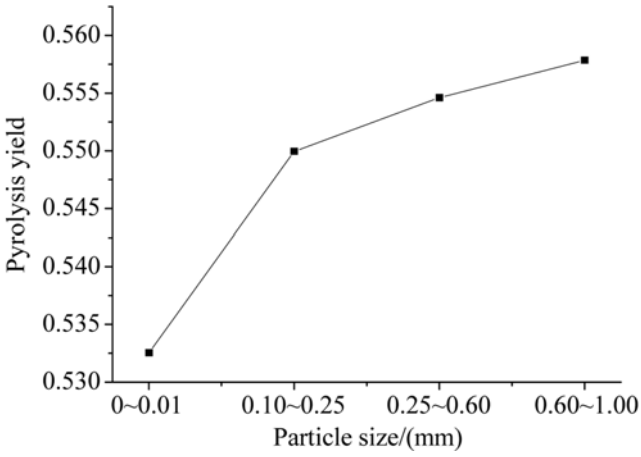

Fig. 13. Pyrolysis yields for various particle sizes.

MECHANISM FUNCTION AND KINETIC PARAMETERS

1. Pyrolysis Kinetics Model

Throughout this paper, t is time, T_0 is the initial absolute temperature of the specimen, T is the specimen's absolute temperature at time t, β is heating rate, A is frequency factor, E is activation energy, R is the gas constant. The pyrolysis conversion α is defined as:

$$\alpha = \frac{W_0 - W_t}{W_0 - W_\infty} \tag{1}$$

where, W_0 is the initial specimen quality, W_t is the specimen quality at time t, and W_∞ is the final quality.

Integration and differential methods are used to derive the basic equations of pyrolysis kinetics:

$$\frac{d\alpha}{dt} = kf(\alpha) \tag{2}$$

$$G(\alpha) = \int_0^\alpha \frac{d\alpha}{f(\alpha)} = kt \tag{3}$$

where $f(\alpha)$ and $G(\alpha)$ are the differential and integration mechanism functions, respectively, k is the rate constant and generally takes the form:

$$k = A\exp(-E/RT) \tag{4}$$

where A is the Arrhenius constant.

With a constant heating rate, β, the following two equations are obtained:

$$T = T_0 + \beta t \tag{5}$$

$$dT = \beta dt \tag{6}$$

The mathematical expression for the differential and integration

can be reformulated by using Eqs. (5) and (6) giving

Differential:

$$\frac{d\alpha}{dT}=\left(\frac{A}{\beta}\right)\exp(-E/RT)f(\alpha) \quad (7)$$

Integration:

$$G(\alpha)=\int_{T_0}^{T}(A/\beta)\exp(-E/RT)dT$$

$$\approx\int_{0}^{T}(A/\beta)\exp(-E/RT)dT=(AE/\beta R)p(u) \quad (8)$$

where u=(E/RT) and , p(u) is an integration function

$$p(u)=\int_{\infty}^{u}-(e^{-u}/u^2)du \quad (9)$$

This integral has no closed expression but has a series expansion

$$p(u)=\frac{e^{-u}}{u^2}\left(1-\frac{2!}{u}+\frac{3!}{u^2}-\frac{4!}{u^3}+\cdots+\frac{(n+1)!}{u^n}+\cdots\right) \quad (10)$$

from which the first term yields the primary approximation of Frank-Kameneskii p(u).

$$p(u)=\frac{e^{-u}}{u^2} \quad (11)$$

Substituting this equation into the integration equation, the Coats-Redfern integration equation can be obtained.

$$\ln(G(\alpha)/T^2)=\ln(AR/\beta E)-E/RT \quad (12)$$

yielding a linear relation between factors $\ln(G(\alpha)/T^2)$ and 1/T. As a consequence, E can be obtained by standard graphical means from the slope and A from the intercept.

By introducing the experimental data into the usual mechanism functions in Table 2 [11] and comparing them in Fig. 14, we select the best linear fit. By dividing the pyrolysis process into low, middle and high temperature ranges, we can calculate E and A of each range by the integration method.

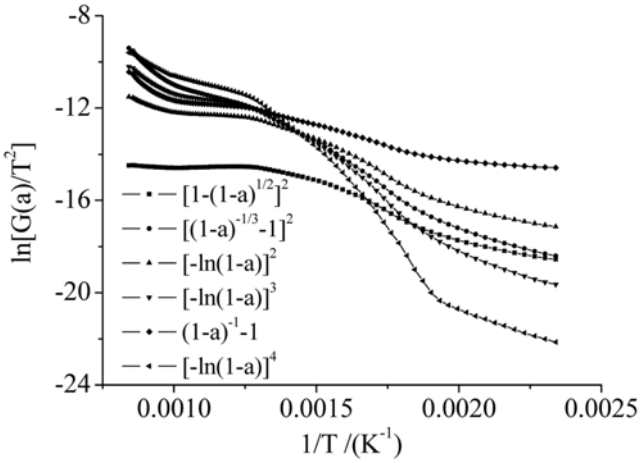

Fig. 14. Profiles of $\ln(G(\alpha)/T^2)-(1/T)$.

In comparing the data of different mechanism functions, we establish the following function dependency:

$$G(\alpha)=(-\ln(1-\alpha))^4 \quad (13)$$

The most probable mechanism function for pyrolysis appears to be best described by the Avrami-Erofeev equation, which represents a random nucleation and consequent growth mechanism function (with an n=4 exponent).

2. Pyrolysis Kinetics Parameters

Because groups of poor thermo-stability split first and subsequently those with stronger thermo-stability, activation energies increase with increasing pyrolysis temperature in low and middle temperature ranges. However, the increase of activation energy of wastes is not as large as that of coal [12] because the time of release of the

Table 2. General functions of kinetic mechanisms

Name	Mechanism	G(a)	f(a)
Jander equation	Two-dimensional diffusion, 2D, n=2	$[1-(1-a)^{1/2}]^2$	$(1-a)^{1/2}[1-(1-a)^{1/2}]^{-1}$
Z-L-T equation	Three-dimensional diffusion, 3D	$[(1-a)^{-1/3}-1]^2$	$1.5(1-a)^{4/3}[(1-a)^{-1/3}-1]^{-1}$
Avrami-erofeev equation	Random nucleus and consequent growth, n=2	$[-\ln(1-a)]^2$	$0.5(1-a)[-\ln(1-a)]^{-1}$
Avrami-erofeev equation	Random nucleus and consequent growth, n=3	$[-\ln(1-a)]^3$	$1/3(1-a)[-\ln(1-a)]^{-2}$
Avrami-erofeev equation	Random nucleus and consequent growth, n=4	$[-\ln(1-a)]^4$	$1/4(1-a)[-\ln(1-a)]^{-3}$
Reaction order	Chemical reaction	$(1-a)^{-1}-1$	$(1-a)^2$

Table 3. Pyrolysis kinetic parameters for various test conditions

	Low (<300 °C)		Middle (300 °C-600 °C)		High (>600 °C)	
	E	A	E	A	E	A
0001-50-1200	71.17	234.46	75.68	2472.01	43.22	4.51
0125-50-1200	65.73	71.62	74.04	2149.45	49.02	9.04
2560-50-1200	63.76	28.91	82.67	10347.55	41.91	3.60
0610-50-1200	69.34	122.32	80.33	6730.71	41.68	3.56
2560-20-1200	50.95	1.24	79.13	2919.10	42.78	1.68
2560-50-1200	63.76	28.91	82.67	10347.55	41.91	3.60
2560-80-1200	58.22	14.62	87.33	45222.40	39.77	4.31

groups overlaps due to too many components in the specimen that interact with each other when being heated. This is the reason changes in activation energies are not so large. In the high temperature ranges, most groups have already finished splitting and only a few unsplit groups remain, thereby activation energy decreases.

For specimen 2560, the activation energy and frequency factors change significantly, and hence it is not possible to establish activation energy rate dependencies in the low temperature range. Activation energy and frequency factors become larger with increasing heating rate. Activation energy increases while frequency factor decreases with the increase of heating rate. For specimens of similar heating rates, the influence of particle size on activation energy is not clear.

CONCLUSIONS

The process of waste pyrolysis has been divided into three stages. The first stage is comprised of the heating period from 40 to 105 ºC and constant temperature of 105 ºC when a specimen loses its external moisture. The second heating period from 105 ºC up to its final temperature with the heating rate of 50 ºC/min constitutes the main pyrolysis stage with an associated large gas release. The constant temperature stage at 1,200 ºC comprises the residual pyrolysis stage characterized by a little weight loss. From the DTG profiles, three obvious peaks in the main pyrolysis stage have been observed with temperatures of 302.3 ºC, 752.2 ºC and 1079.4 ºC, respectively.

We have found that particle size and heating rate have obvious influences on characteristic temperatures, which rise with increasing particle size. The initial weight loss temperature decreases while the initial pyrolysis temperature, the maximum pyrolysis rate temperature and final temperature increase with increasing heating rate.

Final temperature and particle size both have great influences on pyrolysis yields. Polycondensation cannot react completely at the low final temperature of 800 ºC, while it can essentially be completed at 900 ºC. Secondary reactions begin at 1,000 ºC, but are not completed until a temperature of 1,100 ºC is attained. Changes between 1,100 ºC and 1,200 ºC are smaller than that between 800 ºC, 900 ºC and 1,000 ºC.

By introducing the experimental data into the usual mechanism functions and comparing them, a best linear fit was found, $G(\alpha)=(-\ln(1-\alpha))^4$, and values for the activation energy E and Arrhenius constant A have been given for various temperature ranges during the pyrolysis process by the integration method.

For each specimen of the same particle size, activation energies were found to increase with increasing temperature in the low and middle temperature ranges while decreasing in the high temperature range. For each specimen of the same particle size but different heating rates, the influence of heating rate on the activation energies and frequency factors is not clear; activation energies and frequency factors increase with increasing heating rate in middle temperature, and activation energy increases while frequency factor decreases with increasing heating rate at high temperature. For specimens with the same heating rate, the influence of particle size on activation energy is not clear.

NOMENCLATURE

A : frequency factor
E : activation energy [kJ/mol]
R : the gas constant [J/(K·mol)]
T : specimen's absolute temperature at time t [K]
T_0 : initial absolute temperature of specimen [K]
T_f : final temperature [K]
T_{il} : initial weight loss temperature [K]
T_{ip} : initial pyrolysis temperature [K]
T_{max} : maximum weight loss rate temperature [K]
t : time [s]
W_0 : initial specimen quality [mg]
W_t : specimen quality at time t [mg]
W_∞ : final quality [mg]
α : the pyrolysis conversion (see Eq. (1))
β : heating rate [ºC/min]

REFERENCES

1. C. Q. Yang and C. Q. Hu. *Fuel & Chemical Processes*, **35**, 39 (2007).
2. S. J. Yoon, Y. C. Choi and S. H. Lee, *Korean J. Chem. Eng*., **513**, 24 (2007).
3. F. Sevim, F. Demir and M. Bilen, *Korean J. Chem. Eng*., **737**, 23 (2006).
4. Y. S. Park, H. N. Shin and D. H. Lee, *Korean J. Chem. Eng*., **1170**, 20 (2003).
5. Z. Q. Li, C. L. Liu and Z. C. Chen, *Bioresource Technology*, **1016**, 10 (2008).
6. Z. Q. Liu, J. H. Li and Y. F. Nie, *China Environmental Protection Industry*, **12**, 6 (2000).
7. Y. Li and Z. Jun, *Environment Herald*, **2**, 46 (2000).
8. J. H. Sharp and S. A. Wendworth, *Anal. Chem*., **41**, 2061 (1969).
9. F. Juan, G. Jose and M. Encinar, *Journal of Analytical and Applied Pyrolysis*, **67**, 182 (2003).
10. M. Miller-Hagedorn, *Journal of Analytical and Applied Pyrolysis*, **68**, 235 (2003).
11. R. Z. Hu and Q. Z. Shi, *Thermal analysis kinetics*, Science Press, China (2001).
12. S. Hu, A. Jess and M. H. Xu, *Fuel*, **17**, 2780 (2007).